Fe nanoparticles on ZnSe: Reversible temperature dependence of the surface barrier potential

M. Cantoni,[1,*] R. Bertacco,[1] A. Brambilla,[2] M. Finazzi,[2] L. Duò,[2] F. Ciccacci,[2] A. Verdini,[3] L. Floreano,[3] A. Morgante,[3,4] M. Passoni,[5] C. S. Casari,[5,6] and A. Li Bassi[5,6]

[1]*CNISM and LNESS, Dipartimento di Fisica—Politecnico di Milano, Via Anzani 42, 22100 Como, Italy*

[2]*CNISM and LNESS, Dipartimento di Fisica—Politecnico di Milano, Piazza L. Da Vinci 32, 20133 Milano, Italy*

[3]*CNR-IOM, Laboratorio Nazionale TASC, Trieste 34149, Italy*

[4]*Department of Physics, Trieste University, Trieste 34127, Italy*

[5]*Dipartimento di Energia and NEMAS—Center for NanoEngineered Materials and Surfaces, Politecnico di Milano, via Ponzio 34/3, 20133 Milano, Italy*

[6]*Center for Nano Science and Technology @Polimi, Istituto Italiano di Tecnologia, via Pascoli 70/3, 20133 Milano, Italy*

(Received 22 July 2011; revised manuscript received 27 February 2012; published 27 April 2012)

The Fe growth on ZnSe(001) takes place via the initial formation of superparamagnetic nano-islands that subsequently coalesce, giving rise to a continuous film for a nominal thickness of 8 Fe monolayers. For a very low Fe coverage (2 Fe monolayers), we show that the surface barrier potential (i.e. the barrier potential seen by electrons incident on the surface), measured by absorbed current spectroscopy, attains very large values (6.9 eV at room temperature) and dramatically changes as a function of temperature, with an increase of $\sim$1.5 eV from room temperature down to 130 K, largely exceeding similar changes observed in both thin films and nanoparticles. This phenomenon disappears as the thickness increases and is fully reversible with temperature. Nonequilibrium phenomena due to the experimental conditions are present, but are not able to explain the observed data. Inverse photoemission, core level photoemission, x-ray photoemission diffraction, and scanning tunneling microscopy are employed in order to find temperature-dependent properties of the Fe islands: while only minor changes as a function of temperature are present in the electronic band structure, the Fe crystal structure, and the morphology of the islands, a noticeable temperature dependence of the Se segregation through the Fe islands is found.

DOI: 10.1103/PhysRevB.85.155456 PACS number(s): 65.40.gh, 68.60.Dv, 68.55.A−, 73.20.At

I. INTRODUCTION

During the last decades, the study of ferromagnet-semiconductor interfaces has attracted more and more interest due to the possibility of using such structures as injectors or analyzers of spin polarized currents in semiconductors.[1,2] Within the wide choice of available materials, both for the ferromagnet (Fe, CoFe, NiFe, . . .) and the semiconductor (GaAs, Ge, ZnSe, . . .), Fe/ZnSe has been shown to be a promising system.[3] In fact, theoretical calculations demonstrate that, in the case of a perfect two-dimensional symmetry, a very high spin polarization of the injected current can be achieved (>97 %) due to the symmetry constraints of the states involved in the injection from Fe to ZnSe.[4,5] Very recently, electrical spin injection from ferromagnetic Fe(001) into *n*-type ZnSe(001) has been performed using the Schottky barrier that forms at the Fe/ZnSe interface, achieving an electron spin polarization (revealed by the radiative recombination in GaAs after crossing a 0.3-μm-thick ZnSe layer) of 54% at 100 K.[6] In the past few years, many works have been devoted to the study of ultrathin Fe films on ZnSe. In particular, some of the authors[7–10] investigated the electronic and magnetic properties of ultrathin Fe films on ZnSe with thickness ranging from 1 to 30 ML, where 1 ML stands for 1 equivalent monolayer and corresponds to 1.43 Å, the layer spacing of bcc Fe. The picture arising is far from simple: while a metallic behavior is established from very low Fe thickness (1 ML), a ferromagnetic behavior develops only at larger coverage (7–8 ML). Below 7 ML, instead, Fe is superparamagnetic, with a blocking temperature lower than 3.5 $\pm$ 1.5 K.[7] This behavior should be ascribed to the growth mode of Fe on ZnSe(001), as revealed by scanning tunneling microscopy:[8,11] an Fe film corresponding to a nominal thickness of 1 ML is constituted by isolated clusters of several hundreds of atoms, corresponding to flat discs with an average diameter of 30 Å and a maximum thickness of 2 ML. When the Fe coverage increases, the islands become larger, thicker, and more elongated; at 5 ML nominal Fe film thickness, they start to coalesce. Finally, at 7 ML, coalescence is accomplished, and the film presents long-range order. Correspondingly, Fe is superparamagnetic up to 6 ML (each island acts as a superparamagnetic particle) and turns ferromagnetic as soon as it becomes continuous (7 ML).[7,8] The latter case is obviously the most studied, in view of applications in magnetic devices as spin injectors and spin valves, requiring well-defined and stable magnetic states of the Fe electrode.[6,12,13] However, during our investigation, some interesting and unexplored properties of the superparamagnetic case emerged.

In this paper, we report on the unexpected temperature dependence of the surface barrier potential ϕ (i.e. the barrier potential seen by an electron incident on the ZnSe surface), measured by absorbed current spectroscopy, in ultrathin Fe films (from 2 to 8 ML). In particular, we found a very large variation of ϕ in the thinnest film (2 ML, corresponding to a nominal thickness of 2.86 Å): when the sample temperature increases by 100 K, ϕ decreases by more than 1 eV. When Fe becomes thicker, however, this effect is more and more reduced. The behavior we present is fully reversible with temperature, as demonstrated by several cycles of heating-cooling. Moreover, the absolute value of ϕ is interesting in itself: in the 2-ML-thick film, the surface barrier potential is 6.9 eV at room temperature, more than 2 eV larger than the Fe work function (4.7 eV). In the last section, finite-size effects, thermal shifts of the work function, nonequilibrium phenomena induced by the experimental techniques, structural, morphological, and

chemical properties of the Fe overlayer and of the ZnSe substrate are considered, as we look for temperature-dependent effects to be correlated with the observed behavior of ϕ.

II. EXPERIMENTAL

The ZnSe samples have been grown in the Laboratoire de Minéralogie et de Crystallographie de Paris (LMCP) by molecular beam epitaxy.[14] On a highly n-doped GaAs substrate, an intrinsic GaAs buffer layer (1000 Å) was grown, and then an undoped ZnSe overlayer (100 Å) was deposited. A capping layer of amorphous Se (100 Å) was finally added, in order to prevent contamination during exposure to air. The measurements have been made in different ultrahigh vacuum (UHV) systems, with base pressure lower than 3×10^{-10} mbar, all of them equipped with Fe deposition cells, in order to avoid any exposition to air after the Fe growth. After the insertion in the UHV chamber, the Se capping layer was removed by heating the substrate at 450 K for 2 h, and then up to 690 K for 10 min in order to obtain a Zn rich $c(2 \times 2)$ reconstruction.[15] The Fe films, with nominal thickness ranging from 2 to 8 ML as monitored by a calibrated quartz microbalance, were grown by molecular beam epitaxy (MBE) at a rate of $\sim$1 Å/min. The temperature was kept at 450 K during the deposition, in order to obtain an epitaxial growth according to a well-established recipe.[8]

The absorbed current spectroscopy (ACS) and inverse photoemission spectroscopy (IPES) experiments have been performed by employing an integrated system equipped with a 0–30 eV electron gun and a photon detector.[16,17] The measurements have been done at normal incidence, with an electron beam current of $\sim$5 μA and a spot diameter $<$1 mm. Note that the beam spot is largely smaller than the sample surface (10×10 mm^2), so that any contribution to the measured signal due to the sample holder can be excluded.

The angle resolved photoemission spectroscopy (ARPES) and x-ray photoelectron diffraction (XPD) measurements have been made at the ALOISA beamline in the ELETTRA synchrotron radiation laboratory in Trieste, Italy,[18,19] with a flux of $\sim 5 \times 10^{11}$ photons·s^{-1} and a spot size of 30×200 μm^2. The photon energies were 170 and 1100 eV for ARPES and XPD, respectively.

All the measurements have been performed with the bottom of the sample grounded, and the thermal contact with the sample holder was provided by In soldering. The temperature was measured by a thermocouple positioned close to the sample, with an uncertainty of $\pm$5 K.

The scanning tunneling microscopy (STM) measurements have been performed using an Omicron Variable Temperature STM in a UHV chamber connected to the preparation system, equipped with an e-beam evaporator and a quartz microbalance for Fe deposition. Scanning tunneling microscopy images have been acquired at room temperature and at 140 K (using a liquid N_2 cooled sample holder) in constant current mode, with homemade electrochemically etched W tips.

III. RESULTS

In ACS, the incident electrons, having a well-defined energy (E_{beam}) with respect to the Fermi level (E_F) of the substrate, couple with unoccupied states in the conduction band. The ACS signal is defined as the ratio between the current absorbed by the sample and the total current at the entrance of the electron gun. It takes into account both the transmittance of the electron optics, slowly depending on the beam energy E, and the probability of filling an empty state above E_F. For example, the black dotted curve in Fig. 1(a) is the ACS spectrum of a bulk Fe(001) single crystal (s.c.).[20] While the features at E-$E_F > 5$ eV are connected to the electronic band structure, the initial steep onset around 4.7 eV must be ascribed to the surface barrier potential of Fe (ϕ): only the electrons that possess enough energy to overcome such barrier (E-$E_F > \phi$) can couple with the Fe conduction band and produce an ACS signal. From the black dotted curve in Fig. 1, we deduce $\phi =$ 4.7 eV for the Fe s.c., taking the surface barrier potential ϕ as the saddle point in the onset region. The accuracy is $\pm$0.05 eV. This result is in full agreement with the values of the Fe work function (that, in a metal, is coincident with the surface barrier potential) reported in literature.[21]

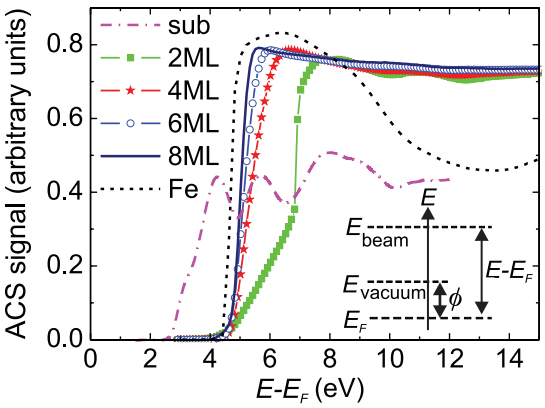

FIG. 1. (Color online) Absorbed current spectroscopy spectra, taken at room temperature, of (i) Fe/ZnSe(001) films with Fe nominal thicknesses of 2, 4, 6, and 8 ML, (ii) a clean ZnSe(001) substrate, and (iii) a bulk Fe(001) single-crystal sample. The ACS signal is defined as the ratio between the current absorbed by the sample and the total current at the entrance of the electron gun. In the inset, the energy scheme for the determination of the surface barrier potential (ϕ) from the ACS spectra is reported.

In Fig. 1 are also reported the room temperature ACS spectra of a clean ZnSe(001) substrate and four Fe/ZnSe(001) samples with different Fe nominal thicknesses ($t_{\text{Fe}} =$ 2, 4, 6, and 8 ML). We note that, while the Fe/ZnSe(001) spectra are essentially similar in the region with E-$E_F > E_M$, where E_M is the position of the first maximum, in the region with E-$E_F < E_M$ a thickness dependence is evident. As a matter of fact, when the Fe thickness increases, the onset shifts towards the Fermi level, and thus ϕ decreases: ϕ result 5.2, 5.1, 5.0, and 4.7 eV for $t_{\text{Fe}} =$ 4, 6, 8 ML, and for the bulk Fe s.c., respectively (the 2-ML-thick film will be discussed later). The decrease of ϕ while increasing t_{Fe} is also accompanied by an increase of the onset slope, defined as the first derivative calculated in the saddle point: as t_{Fe} becomes larger, the onset becomes steeper, and finally, at $t_{\text{Fe}} = 8$ ML, it reaches the Fe s.c. slope. Anyway, despite the latter evidence and even if the 8-ML-thick Fe film is fully coalesced,[8] some differences are

present with respect to Fe s.c.: for all thicknesses, ϕ is larger in Fe/ZnSe than in Fe s.c ($\phi_{Fe/ZnSe}$-$\phi_{Fes.c.} \geqslant 0.3$ eV), and the ACS spectrum of Fe/ZnSe is definitely less featured than that of Fe s.c., indicating a worse quality of the Fe thin film with respect to Fe s.c. As we discussed in Ref. 8, these findings can be ascribed to an Se segregation within Fe, to the presence of a floating Se overlayer, and/or to a poor crystalline quality of the Fe film and of the interface with ZnSe.

Coming to the 2-ML-thick Fe/ZnSe film, we immediately note that, at room temperature, the onset region can be clearly divided into two distinct parts: between 4.4 and 6.8 eV, the absorbed current increases smoothly with a linear trend (the slope is around 1/3 of that of the 4-ML film), while, between 6.8 and 7 eV, it is steeper, with the same slope of the bulk Fe curve at the onset. The value of ϕ, estimated as the saddle point in the latter region, is 6.9 eV. Above 7 eV, the 2-ML-thick film does not present relevant differences with respect to thicker films, apart from the presence of two features, at about 8 and 11 eV: these are also present in the spectrum from the clean ZnSe, so that we can ascribe them to uncovered regions of the substrate. In the following, we will concentrate on the onset region (i.e. below the first maximum), where the Fe thickness dependence is more evident.

Figures 2(a) and 2(b) report the ACS spectra of Fe/ZnSe films with 2- and 6-ML Fe thicknesses, respectively, as a function of the temperature (T). We underline the fact that all the observed temperature-dependent behaviors are fully reversible with T: several cooling-heating cycles do not change

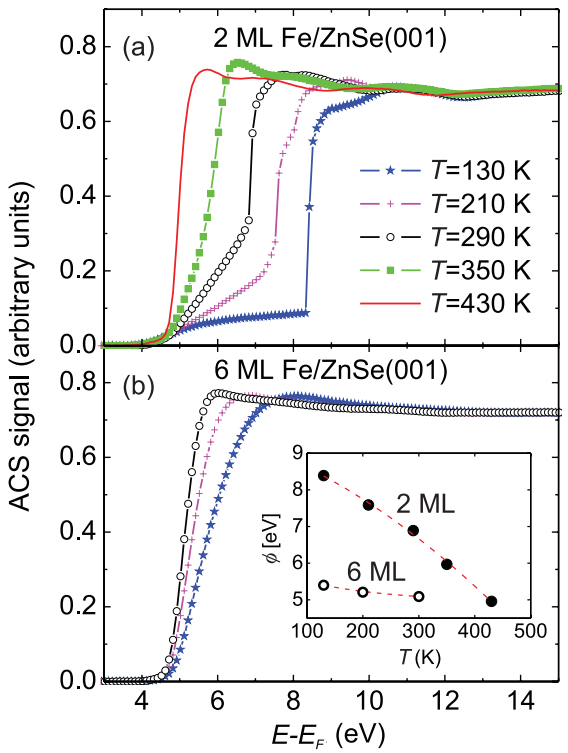

FIG. 2. (Color online) Absorbed current spectroscopy spectra of Fe/ZnSe(001) films with nominal thicknesses of (a) 2 and (b) 6 ML, measured at different temperatures. In the inset of (b), the surface barrier potentials (ϕ) are reported as a function of the temperature (the red dashed lines are only guides for the eye).

TABLE I. Surface barrier potential values for 2- and 6-ML-thick Fe films on ZnSe(001), at different temperatures, measured by absorbed current spectroscopy.

2 ML		6 ML	
T (K)	ϕ (eV)	T (K)	ϕ (eV)
130	8.40	130	5.40
210	7.60	200	5.20
290	6.90	300	5.10
350	5.95		
430	4.95		

both the temperature dependence of the ACS spectra and the measured ϕ values. For both thicknesses reported in Fig. 2, an increase of T is accompanied by a decrease of ϕ, as shown in Table I and in the inset of Fig. 2(b).

We start considering the 2-ML-thick Fe/ZnSe film reported in Fig. 2(a). The curves measured from $T = 130$ K (low temperature, LT) to $T = 290$ K (room temperature, RT) show a double onset, i.e. the onset region can be divided into two distinct parts as discussed above. At higher temperatures (up to 430 K), instead, a single onset is present. From Fig. 2(a) and Table I, two relevant facts come out. (i) The value of ϕ, estimated on the stepped part of the onset, is far higher than expected: at RT, it exceeds the Fe work function (4.7 eV[21]) by 2.2 eV, and the ZnSe electron affinity (3.5 eV[22]) by 3.4 eV. (ii) The range of variation of ϕ is particularly large: ϕ decreases by $\Delta\phi = 1.5$ eV when the sample is heated from 130 to 290 K, and by 3.4 eV from 130 to 430 K. The derivative $d\phi/dT$ (evaluated on ACS spectra spaced by 20 K from 130 to 430 K, not reported) is -11 ± 0.7 meV/K, almost constant in the considered temperature range.

We now move to the 6-ML-thick film reported in Fig. 2(b). The Fe films with nominal thickness of 4 and 8 ML (not shown) present the same temperature-dependent behavior as the 6-ML-thick film, so we take the latter as representative of the 4–8-ML thickness range. At variance with the 2-ML-thick film, here, the ACS curve presents a single onset. Moreover, $\Delta\phi$ is considerably smaller than in the 2-ML-thick film case: it is 0.3 eV (corresponding to 1/5 of the 2-ML-thick film value) when the sample is heated from 130 to 300 K, and $d\phi/dT$ is -1.8 ± 0.4 meV/K (about 1/6 of the same quantity in the 2-ML-thick film).

Summarizing this section, we showed that, for very thin Fe films (2 ML), the surface barrier potential ϕ attains very large values ($\phi = 6.9$ eV at room temperature) and presents a dramatic temperature dependence, with an increase of $\Delta\phi \sim 1.5$ eV from room temperature down to 130 K. When the Fe thickness increases, both ϕ and $\Delta\phi$ decrease, approaching the values of a bulk Fe film; by the contrary, the Fe work function (4.7 eV) is not attained even when the full coalescence is accomplished ($\phi = 5$ eV for a 8 ML thick Fe film).

IV. DISCUSSION

As reported in Refs. 8 and 23, a Fe/ZnSe film with a nominal thickness of 2 ML is constituted by isolated clusters of several hundreds of atoms, leaving part of the ZnSe substrate

uncovered by Fe. As a consequence, both Fe and ZnSe regions are exposed to the electron beam and contribute to the ACS and IPES spectra discussed in Sec. III. The double onset in the 2-ML-thick film reported in Fig. 1 is characteristic of the presence of these two regions. From the hierarchy of the work functions, the smooth initial part of the onset might be associated with the uncovered ZnSe, while the steep slope might be due to the Fe islands. However, the interpretation of the measured ϕ value as an average between the Fe work function and the ZnSe electron affinity is not appropriate: as a matter of fact, ϕ is 6.9 eV on the 2-ML-thick film at RT, that is larger than both the Fe work function (4.7 eV) and the ZnSe electron affinity (3.5 eV). Additional explanations for the observed behaviors must thus be looked for. In the next sections, different mechanisms will be considered: thermal effects in the Fe overlayer, nonequilibrium phenomena (reverse bias Schottky diode and surface electron-in voltage effects), modifications of the Fe crystal structure and of the islands' morphology, finite-size effects, and chemical intermixing or segregation.

A. Thermal work function shift

The thermal work function shift of metal surfaces (polycrystalline and continuous), reported in Ref. 24, is a possible explanation for the temperature dependence of ϕ. Neglecting for simplicity any crystal structure and finite-size effect, the work function of Fe (φ) can be expressed as:

$$\varphi = \text{constant} - 0.6 \times 10^{-5} T - 7.4 \times 10^{-8} T^2 \qquad (1)$$

where φ and T are in eV and K, respectively. The determination of the constant is nonessential because we are interested in $\Delta\varphi = \varphi$ (130 K) $-$ φ (RT). From Eq. (1), we obtain $\Delta\varphi = 5.9$ meV, more than two orders of magnitude smaller than the value measured on the 2-ML-thick film, $\Delta\phi = 1.5$ eV. Then, apart from an almost negligible contribution, the thermal dependence of φ cannot explain the behavior of ϕ as a function of temperature.

B. Nonequilibrium phenomena

In nonequilibrium phenomena, schematized in Fig. 3(a), the Fermi level of the substrate (E_F^{ZnSe}) and of the Fe film (E_F^{Fe}) can be misaligned. The surface barrier potential of Fe (ϕ_{Fe}) is defined as the difference between the vacuum level (VL) and the Fermi energy (E_F) of Fe, while the surface barrier potential measured by ACS (ϕ_{ACS}) is the difference between the vacuum level of Fe and E_F of the substrate. From Fig. 3(a), the misalignments of the Fermi levels can be calculated as $\Delta E_F = E_F^{\text{Fe}} - E_F^{\text{ZnSe}} = \phi_{\text{ACS}} - \phi_{\text{Fe}}$. In the 2-ML-thick Fe/ZnSe film, they result $\Delta E_F = 3.7$ eV at 130 K, $\Delta E_F = 2.2$ eV at room temperature, and $\Delta E_F = 0.3$ eV at 430 K (see Table I).

We individuated two possible nonequilibrium mechanisms that can act in the Fe/ZnSe sample: (i) the band bending due to the Schottky barrier between Fe and ZnSe and (ii) the surface electron-in voltage effect due to the electron-hole pairs generated in ZnSe by the incident beam.

A Schottky barrier naturally develops at the interface between Fe and ZnSe, producing a band bending as in Fig. 3(c).[8] In equilibrium (the ZnSe bands are represented with

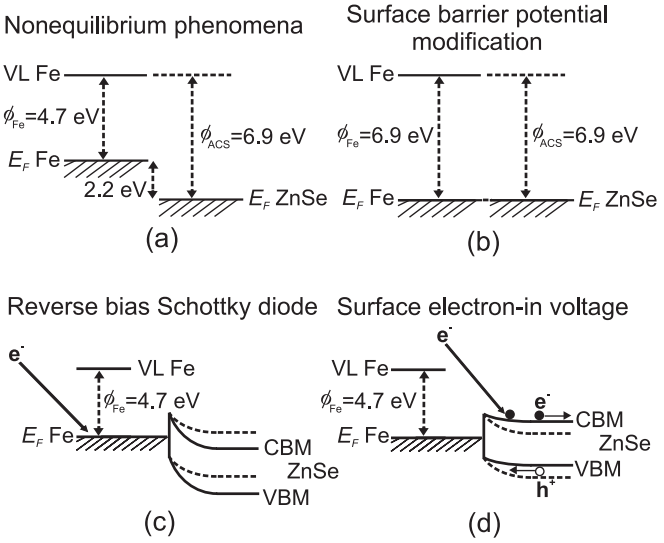

FIG. 3. Mechanisms in play for explaining the surface barrier potential data: (a) nonequilibrium phenomena, giving rise to a misalignment of the Fe and ZnSe Fermi levels, and (b) surface barrier potential modification. Among the nonequilibrium phenomena, two mechanisms are considered: (c) reverse biased Schottky diode behavior and (d) surface electron-in voltage in ZnSe.

dashed lines), without external perturbations (e.g. the incident electron beam), the Fermi levels of Fe and ZnSe are coincident, so that $\Delta E_F = 0$ and $\phi_{\text{ACS}} = \phi_{\text{Fe}}$. During ACS and IPES measurements, instead, the electrons absorbed by the Fe layer will move towards the ZnSe, thus creating a negative current from Fe to ZnSe, so that the sample will behave as a Schottky diode in reverse bias. In this situation, the band bending will increase (the ZnSe bands are represented with continuous lines), the Fermi level of the substrate will drop with respect to that of Fe ($E_F^{\text{ZnSe}} < E_F^{\text{Fe}}$), ΔE_F will be positive, and ϕ_{ACS} will be larger than ϕ_{Fe}. When the temperature is reduced, a further increase of the band bending is expected, according to the Schottky model:[25] ΔE_F and ϕ_{ACS} will increase, in agreement with the trend of Table I. At the same time, the whole band structure of Fe will shift by ΔE_F because the band structure of ZnSe is fixed by the condition $E_F^{\text{ZnSe}} = 0$ (the substrate is grounded).

In order to quantitatively determine this shift, we consider the inverse photoemission spectroscopy (IPES) spectra reported in Fig. 4 for the 2-ML-thick Fe film at 130 and 290 K. Inverse photoemission spectroscopy is an electron-in, photon-out technique, employed for mapping the conduction band of the sample. The IPES experiments reported in this paper are made at normal incidence, so that the probed states are along the ΓH and ΓX lines of the Brillouin zones of ZnSe(001) and Fe(001), respectively. In Fig. 4, two main features are evident above E_F: a shoulder at 1.5 eV ($B_{1,2}$) and a peak at 6.5 eV (B). Here, $B_{1,2}$ is the superposition of the peaks B1 and B2 of Fe, corresponding to transitions towards final states (majority- and minority-spin states, respectively) close to the H'_{25} point of the Fe bulk band structure.[8] B, instead, is attributed to transitions between unoccupied bulk Δ bands along the ΓX line in the first Brillouin zone of ZnSe.[26] When the temperature is reduced from 290 to 130 K,

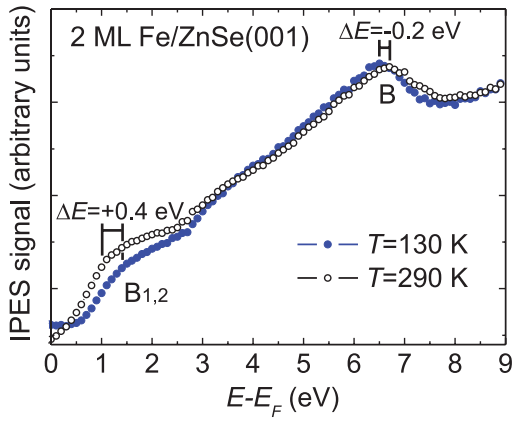

FIG. 4. (Color online) Inverse photoemission spectroscopy spectra of an Fe/ZnSe(001) film with a nominal thickness of 2 ML, measured at 130 K (full dots) and 290 K (empty dots).

B and $B_{1,2}$ shift by $\Delta E = -0.2$ and $+0.4$ eV, respectively. We consider the behavior of $B_{1,2}$, which is associated to Fe and is thus representative of the shift of the Fe band structure. The behavior of $B_{1,2}$, moving away from the Fermi level when T decreases, is in agreement with the Schottky theory: a rigid shift of the Fe band structure can therefore be deduced. Anyway, IPES measures a shift of 0.4 eV only from RT to LT, more than four times smaller than expected from ACS data ($\Delta\phi = 1.5$ eV), so that this nonequilibrium mechanism cannot completely explain the experimental results.

The second mechanism we consider is the surface electron-in voltage effect, schematized in Fig. 3(d).[27] The electron beam incident on the sample will excite electron-hole pairs in the depletion region of the ZnSe, close to the interface with Fe. The electric field in this region will separate the pairs, so that the holes will flow towards Fe and the electrons towards ZnSe. This effect will partially compensate the charges accumulated in the depletion region, so that the band bending will decrease. Such a mechanism, flattening the bands as in Fig. 3(d), will raise the Fermi level of the substrate with respect to that of Fe ($E_F^{\mathrm{ZnSe}} > E_F^{\mathrm{Fe}}$), giving a negative ΔE_F, in contrast with our experimental results. Moreover, because the ability of the sample to discharge the electrons in excess will be reduced at lower temperature, the band flattening will increase, ΔE_F will become more negative, and the measured surface barrier potential ($\phi_{\mathrm{ACS}} = \phi_{\mathrm{Fe}} + \Delta E_F$) will decrease, instead of increasing as in Table I. We then conclude that the surface electron-in voltage effect is not responsible for any rigid shift of the Fe band structure.

On the other hand, we note that the surface electron-in voltage effect can be put in relation with the shift of the B peak, associated with the ZnSe band structure,[27] reported in Fig. 4. Moving towards the Fermi level when T decreases, this shift is compatible with the surface electron-in voltage mechanism that we previously demonstrated (see Ref. 27) to be mainly responsible for nonequilibrium band bending in a ZnSe substrate (in this case, the part of the ZnSe substrate not covered by the Fe islands).

To summarize this section, the surface electron-in voltage effect completely disagrees with the observed temperature dependence of ϕ, while the Schottky model of the Fe/ZnSe interface under reverse bias predicts the right trend, but it is quantitatively not enough for fitting the measured $\Delta\phi$.

As a matter of fact, if $\Delta\phi$ was completely due to surface barrier potential modifications [$\phi_{\mathrm{ACS}} = \phi_{\mathrm{Fe}}$ as in Fig. 3(b), and thus $\Delta\phi = \phi_{\mathrm{Fe}}(\mathrm{LT})$-$\phi_{\mathrm{Fe}}(\mathrm{RT})$] and not to nonequilibrium phenomena induced by the experimental conditions, then the band structure would be unaffected, and no shifts of the Fe peaks in IPES would be expected. Since, on the contrary, a shift is observed (the shoulder $B_{1,2}$ moves by 0.4 eV), we can conclude that the observed $\Delta\phi$ (1.5 eV) is the sum of two contributions: (1) a nonequilibrium band bending as in a reverse-biased Schottky diode ($\Delta\phi_1 = 0.4$ eV) and (2) a variation of ϕ_{Fe} with respect to the bulk value ($\Delta\phi_2 = 1.1$ eV). In the following sections, different mechanisms will be considered for explaining this second contribution.

C. Fe structure

The surface barrier potential of a metal is dependent on the surface structure, e.g. different surface orientations produce different surface potentials,[28] and an increase of the surface lattice constant at the surface is predicted to reduce the total surface dipole.[29] Any temperature-dependent structural variation of the Fe structure as a function of the temperature has been looked for by x-ray photoelectron diffraction. In Fig. 5, the XPD anisotropy is shown for films with different nominal thicknesses (2, 4, and 6 ML) at two different temperatures, 150 K (empty dots) and 300 K (full dots). The intensities of the Fe $2p_{3/2}$ peak, excited by photons with $h\nu = 1100$ eV, were recorded at different polar angles of emission from the surface, with the sample oriented along the [110] azimuth.

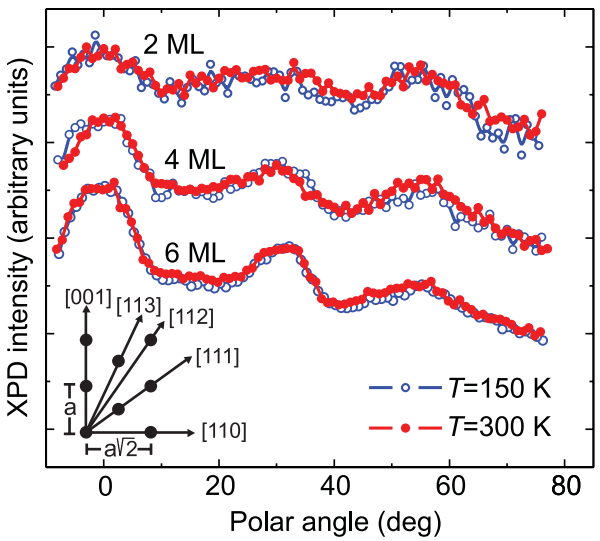

FIG. 5. (Color online) X-ray photoelectron diffraction polar scans measured on Fe/ZnSe(001) films with nominal thicknesses of 2 (top), 4 (center), and 6 ML (bottom) at two different temperatures, 150 K (empty dots) and 300 K (full dots). The intensities of the Fe $2p_{3/2}$ peak, excited by photons with $h\nu = 1100$ eV, were recorded at different polar angles of emission from the surface, with the sample oriented along the [110] azimuth. In the inset, the main forward scattering directions are indicated.

In a forward-scattering picture (see the inset of Fig. 5), the peaks at 0° and ∼55° are ascribed to scattering along the [001] and [111] crystallographic directions. While two layers of Fe are enough for producing forward scattering along the [111] direction, at least three layers are needed for having a peak along the [001] orientation. This indicates that, in the film with nominal thickness of 2 ML, local regions with thickness of at least three layers must be present. The peak at ∼30°, instead, is produced by the superposition of the peaks at 25.2° and 35.3° polar angles that are due to scattering along the [113] and [112] directions, respectively. As shown in the inset of Fig. 5, these peaks require local thicknesses larger or equal to four and five layers, respectively. The more the nominal thickness of the film increases, the more the peak at ∼30° emerges, as reasonably expected; anyway, we note that it is already present in the 2-ML-thick film, thus confirming that the Fe film is made by island, with height up to five layers, and not by a layer of constant thickness.[7,8,11]

Coming to the temperature dependence, we considered the possibility of a temperature dependent reaggregation of the Fe atoms into islands of different dimensions, as reported, for instance, in Fe/Cu_3Au.[30] However, from Fig. 5, we note that the LT and RT cases are rather equivalent, within the accuracy of the XPD technique: we can thus rule out any relevant structural modification induced by temperature variations.

D. Fe morphology and finite-size effects

The Fe morphology has been investigated by STM as a function of temperature. Figure 6 reports the images of the 2-ML-thick Fe film measured at 300 K (a) and 140 K (b). In agreement with the literature,[8,11] STM shows that the film is made of islands with circular or elliptical shapes and area ranging from 20 to 40 nm^2, and the average number of atoms in each island is about 500–1000. The coverage of the Fe islands is larger than 70% of the substrate area. Looking at the temperature dependence, we considered the possibility of a temperature-driven change of morphology of the Fe islands, as reported, for example, in Fe/GaAs.[31] However, the comparison between (a) and (b) of Fig. 6 did not reveal any evident morphological difference, nor in the size or in the shape, so that even this effect can be ruled out.

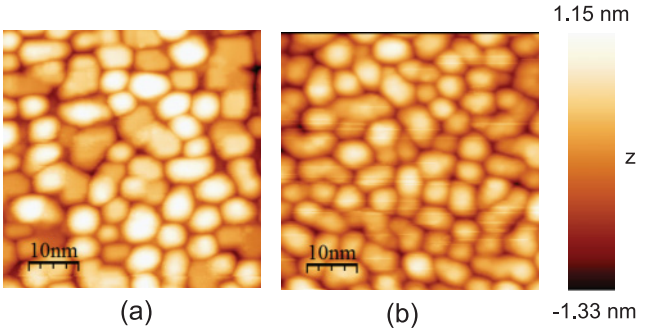

FIG. 6. (Color online) Scanning tunneling microscopy images (50 × 50 nm^2) of an Fe/ZnSe(001) film with a nominal thickness of 2 ML, measured in constant current mode at (a) 300 K (I = 1 nA; V = 1 V) and (b) 140 K (I = 1 nA; V = 0.05 V).

It is known that the finite dimensionality modifies the work function of a metal with respect to the bulk. By using the model reported in Ref. 32, we estimated the work function of a cluster made by 500–1000 atoms. We made two approximations: (i) the islands were considered equivalent to spherical clusters, and (ii) the electron removal energy of the Fe clusters, estimated by the model, was identified with the surface barrier potential. The Fe work function (W = 4.7 eV)[21] and the values reported in Ref. 32 for the atomic polarizability and the cutoff parameter of Fe were employed for the calculations. The resulting ϕ was ∼5.1 eV, 1.8 eV smaller than the observed value of 6.9 eV at RT. In order to obtain the latter value, instead, we would need clusters made by only 6–7 atoms, far below the experimental value of several hundreds of atoms. We then conclude that finite-size effects alone can not justify the observed values of the surface barrier potential.

E. Chemical intermixing and segregation

Finally, temperature-dependent chemical effects have been investigated. In Ref. 8, we showed by x-ray photoemission spectroscopy (XPS) that an Se segregation towards the Fe surface takes place in Fe/ZnSe samples grown with the same procedure employed in this paper. This phenomenon has already been observed in other systems, like FePd/ZnSe[33] and Fe/CdSe.[34] In order to evidence a temperature dependence of this Se segregation, we measured by photoemission spectroscopy (PES), with a photon energy $h\nu$ = 170 eV, the Se3d and Zn3d core levels of the 2-ML-thick Fe/ZnSe film at 150 K (LT) and 300 K (RT), as shown in Fig. 7(a). While the

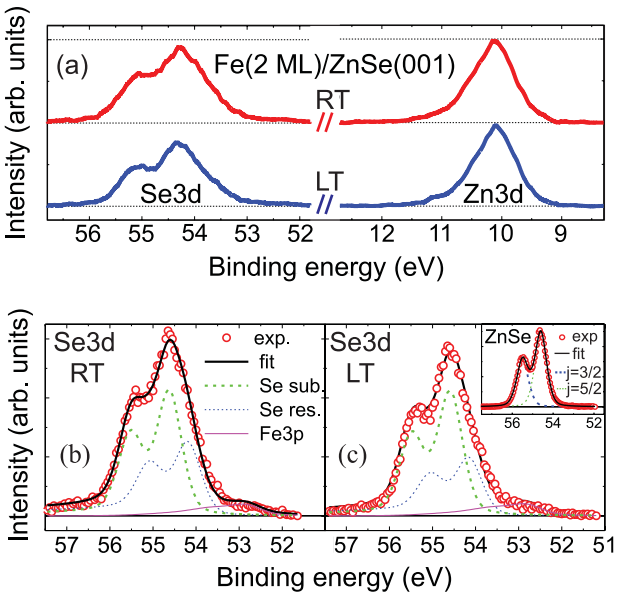

FIG. 7. (Color online) X-ray photoemission spectroscopy spectra, measured with a photon energy $h\nu$ = 170 eV, of a Fe/ZnSe(001) film with a nominal thickness of 2 ML: (a) Se3d and Zn3d at RT (300 K) and LT (150 K); Se3d peak at (b) RT and (c) LT fitted by a substrate component, a residual component, and the Fe3p contribution. An integral background due to the secondary electrons has been previously subtracted. The form of each of the Se contributions has been taken from the Se3d spectrum measured on a clean ZnSe(001) substrate [see the inset of (c)].

intensity of the Zn3*d* level is independent from temperature, the intensity of the Se3*d* level is not. As a matter of fact, the measured Zn3*d*/Se3*d* intensity ratios, normalized to the respective photoemission cross sections, are 1 (in agreement with Ref. 8) and 0.8 at RT and LT, respectively: when the temperature is reduced, the intensity of the Se peak decreases. We found that the same behavior takes place in thicker films (data not shown).

A fitting procedure has been applied to the Se3*d* peaks reported in Fig. 7(a): the results are shown in Figs. 7(b) and 7(c) for the RT and LT situations, respectively. An integral background due to the secondary electrons has been subtracted from both the spectra. In order to improve the reliability of the fitting procedure, we measured the Se3*d* feature on a clean ZnSe substrate, as shown in the inset of Fig. 7(c), and we fitted it by two identical line shapes, corresponding to the Se3$d_{3/2}$ and Se3$d_{5/2}$ components, each one being the convolution of a Doniach–Sunjic function[35] and a Gaussian curve. Then, we employed the so-obtained curves for fitting the Se3*d* peak in the Fe/ZnSe film. The Se signal was taken as the sum of two distinct contributions, one placed in the nominal position and ascribed to the contribution from the substrate, and the second attributed to the residual Se, i.e. not incorporated into the substrate. The Fe3*p* peak, being partially superimposed to Se3*d*, has been introduced by taking its shape from literature data[36] and by fixing its position at the nominal value with respect to the Zn3*d* peak. From the fit, the residual Se component resulted shifted by $\Delta E = 0.44$ eV towards lower binding energies with respect to the substrate component. The direction of this shift is compatible with the existence of an Fe_xSe_y alloy, even if the precise stoichiometry can not be assessed from the observed data.[37] When the temperature was reduced from RT to LT, the ratio between the residual and the substrate Se components decreased from 0.7 to 0.6, while the Fe signal remained essentially unchanged. This result agrees with Fig. 7(a): the Se segregation increases with temperature. Being the only relevant temperature-dependent property we found, Se segregation is likely to be the candidate for explaining the results of Sec. III. Anyway, this is definitely beyond the scope of this paper because it would require a more complex analysis of the Fe_xSe_y alloy properties, as the stoichiometry and the local distribution (uniform or by clusters, embedded into or floating over the Fe islands), not accessible by the present data.

V. CONCLUSIONS

In this paper, we studied the surface barrier potential ϕ in ultrathin Fe films grows on ZnSe(001) by molecular beam epitaxy. We found that, for a very low Fe coverage (2 Fe monolayers), the surface barrier potential, measured by absorbed current spectroscopy, attains very large values ($\phi = 6.9$ eV at room temperature) and dramatically changes as a function of temperature, with an increase of $\Delta\phi \sim 1.5$ eV from room temperature down to 130 K. These films are made by Fe islands with area ranging from 20 to 40 nm^2 and containing about 500–1000 Fe atoms. Only above 70% of the substrate is covered by Fe. When the Fe thickness increases, both ϕ and $\Delta\phi$ decrease, approaching the values of a bulk Fe film, even if the Fe work function (4.7 eV) is not attained when the full coalescence is accomplished ($\phi = 5$ eV for an 8-ML-thick Fe film).

We showed that neither the temperature dependence of the Fe work function, nor the nonequilibrium phenomena induced by the experimental techniques, nor the finite-size effect of Fe islands can account for the observed behavior of ϕ. Inverse photoemission, x-ray photoemission diffraction, and scanning tunneling microscopy show minor changes in the electronic band structure, Fe crystal structure, and islands' morphology as a function of temperature, while core level photoemission reveals that an Fe_xSe_y alloy is formed, and its intensity, relative to Se, shows a noticeable temperature dependence.

ACKNOWLEDGMENTS

We are very grateful to M. Marangolo, M. Eddrief, and V. H. Etgens for providing the ZnSe substrates, to P. Biagioni, M. Portalupi, M. Riva, and the staff of the ALOISA beamline for their help in the spectroscopy measurements, to D. Cattaneo, S. Foglio, and F. Donati for their help in STM measurements and data analysis, and to M. Leone for his skillful technical assistance.

*Corresponding author: matteo.cantoni@polimi.it

[1] M. E. Flatte and G. Vignale, Appl. Phys. Lett. **78**, 1273 (2001).
[2] I. Zŭtic, J. Fabian, and S. Das Sarma, Phys. Rev. Lett. **88**, 066603 (2002).
[3] F. Gustavsson, J. M. George, V.H. Etgens, and M. Eddrief, Phys. Rev. B **64**, 184422 (2001).
[4] Ph. Mavropoulos, N. Papanikolaou, and P. H. Dederichs, Phys. Rev. Lett. **85**, 1088 (2000).
[5] O. Wunnicke, Ph. Mavropoulos, R. Zeller, P. H. Dederichs, and D. Grundler, Phys. Rev. B **65**, 241306R (2002).
[6] A. T. Hanbicki, G. Kioseoglou, M. A. Holub, O. M. J. Van't Erve, and B. T. Jonker, Appl. Phys. Lett. **94**, 082507 (2009).
[7] M. Cantoni, R. Bertacco, F. Ciccacci, E. Puppin, E. Pinotti, M. Brenna, M. Marangolo, M. Eddrieff, P. Torelli, F. Maccherozzi, J. Fujii, and G. Panaccione, J. Magn. Magn. Mater. **316**, e545 (2007).
[8] R. Bertacco, M. Riva, M. Cantoni, F. Ciccacci, M. Portalupi, A. Brambilla, L. Duò, P. Vavassori, F. Gustavsson, J. -M. George, M. Marangolo, M. Eddrief, and V. H. Etgens, Phys. Rev. B **69**, 054421 (2004).
[9] M. Portalupi, R. Bertacco, M. Cantoni, A. Brambilla, M. Riva, L. Duò, and F. Ciccacci, J. Magn. Magn. Mater. **272–276**, 1907 (2004).
[10] A. Brambilla, L. Duò, M. Cantoni, M. Riva, R. Bertacco, M. Portalupi, and F. Ciccacci, Solid State Commun. **135**, 158 (2005).
[11] M. Marangolo, F. Gustavsson, G. M. Guichar, M. Eddrief, J. Varalda, V. H. Etgens, M. Rivoire, F. Gendron, H. Magnan, D. H. Mosca, and J. M. George, Phys. Rev. B **70**, 134404 (2004).
[12] D. Bilic, E. Dan Dahlberg, A. Chaiken, C. Gutierrez, P. Lubitz, J. J. Krebs, M. Z. Harford, and G. A. Prinz, J. Appl. Phys. **75**, 7073 (1994).

[13]H. Saito, S. Yuasa, K. Ando, Y. Hamada, and Y. Suzuki, Appl. Phys. Lett. **89**, 232502 (2006).
[14]L. Carbonell, V. H. Etgens, A. Kobel, M. Eddrief, and B. Capelle, J. Cryst. Growth **201/202**, 502 (1999).
[15]W. Chen, A. Kahn, P. Soukiassian, P. S. Mangat, J. Gaines, C. Ponzoni, and D. Olego, Phys. Rev. B **49**, R10790 (1994).
[16]R. Bertacco, M. Cantoni, M. Riva, A. Tagliaferri, and F. Ciccacci, Appl. Surf. Sci. **252**, 1754 (2005).
[17]M. Cantoni and R. Bertacco, Rev. Sci. Instrum. **75**, 2387 (2004).
[18]L. Floreano, G. Naletto, D. Cvetko, R. Gotter, M. Malvezzi, L. Marassi, A. Morgante, A. Santaniello, A. Verdini, F. Tommasini and G. Tondello, Rev. Sci. Instrum. **70**, 3855 (1999).
[19]R. Gotter, A. Ruocco, A. Morgante, D. Cvetko, L. Floreano, F. Tommasini, and G. Stefani, Nucl. Intrum. Methods A **467-468**, 1468 (2001).
[20]R. Bertacco, S. De Rossi, and F. Ciccacci, J. Vac. Sci. Technol. A **16**, 2277 (1998).
[21]K. Wong, S. Vongehr, and V.V. Kresin, Phys. Rev. B **67**, 035406 (2003).
[22]F. Xu, M. Vos, J. H. Weaver, and H. Cheng, Phys. Rev. B **38**, 13418 (1988).
[23]M. Marangolo, F. Gustavsson, G. M. Guichar, M. Eddrief, J. Varalda, V. H. Etgens, M. Rivoire, F. Gendron, H. Magnan, D. H. Mosca, and J. M. George, Phys. Rev. B **70**, 134404 (2004).
[24]T. Durakiewicz, A. J. Arko, J. J. Joyce, D. P. Moore, and S. Halas, Surf. Sci. **478**, 72 (2001).
[25]M. Sze and K. K. Ng, *Physics of Semiconductor Devices* (John Wiley & Sons, Hoboken, New Jersey, USA, 2007).
[26]H. Dröge, M. Nagelstraßer, J. Nürnberger, W. Faschinger, A. Fleszar, and H.-P. Steinrück, Surf. Sci. **454**, 477 (2000).
[27]M. Cantoni, R. Bertacco, A. Brambilla, and F. Ciccacci, J. Electron Spectrosc. Relat. Phenom. **173**, 84 (2009).
[28]M. Grass, J. Braun, G. Borstel, R. Schneider, H. Durr, T. Fauster, and V. Dose, J. Phys.: Condens. Matter **2001**, 599 (1993).
[29]G. Paasch, H. Eschrig, and W. John, Phys. Status Solidi B **51**, 283 (1972).
[30]A. Verdini, L. Floreano, F. Bruno, D. Cvetko, A. Morgante, F. Bisio, S. Terreni, and M. Canepa, Phys. Rev. B **65**, 233403 (2002).
[31]K. Zakeri, C. Urban, T. Kebe, J. Lindner, U. Köler, and M. Farle, Appl. Phys. A **90**, 487 (2008).
[32]K. Wong, S. Vongehr, and V. V. Kresin, Phys. Rev. B **67**, 035406 (2003).
[33]C. Bourgognon, S. Tatarenko, J. Cibert, L. Carbonell, V. H. Etgens, M. Eddrief, B. Gilles, A. Marty, and Y. Samson, Appl. Phys. Lett. **76**, 1455 (2000).
[34]B. A. Orlowski, J. P. Lacharme, and C. A. Sebenne, Appl. Surf. Sci. **56**, 224 (1992).
[35]P. A. Bruhwiler and S. E. Schnatterly, Phys. Rev. Lett. **61**, 357 (1988).
[36]G. Rossi, G. Panaccione and F. Sirotti, Phys. Rev. B **54**, 4080 (1996).
[37]N. Hamdadou, J. C. Bernède, and A. Khelil, J. Cryst. Growth **241**, 313 (2002).